Scaling and resonances in elementary $K^+\Lambda$ photoproduction

R. A. Schumacher[1] and M. M. Sargsian[2]
[1]*Department of Physics, Carnegie Mellon University, Pittsburgh, Pennsylvania 15213, USA*
[2]*Department of Physics, Florida International University, Miami, Florida 33199, USA*
(Received 10 December 2010; published 28 February 2011)

Recent cross-section data for the reaction $\gamma + p \to K^+ + \Lambda$ are examined for evidence of scaling in both the low-t Regge domain and in the high-$\sqrt{s}$ and $-t$ domain where constituent counting may apply. It is shown that the reaction does scale in both regimes. At large center-of-mass angles, s^{-7} scaling appears to hold at essentially all $-t$ but with angle-dependent oscillations. The scaled data show particularly strong evidence for s-channel resonances for $-t$ below 2 GeV^2 and for W below about 2.3 GeV. The dominant contributions are consistent with an N^*S_{11} resonance at 1690 MeV, a P_{13} resonance at 1920 MeV, and a D_{13} resonance at 2100 MeV, which interfere to give the observed strong angular dependence.

DOI: 10.1103/PhysRevC.83.025207 PACS number(s): 25.20.Lj, 13.40.−f, 13.60.Le, 14.20.Gk

I. INTRODUCTION

In the GeV energy domain, there are competing pictures for how meson photoproduction reactions can be most economically described. In the meson-baryon picture, pseudoscalar meson photoproduction proceeds by s- and u-channel baryon exchange, plus t-channel meson exchange. At $|-t| < 1$ GeV^2 and high W ($=\sqrt{s}$), cross sections are frequently well described in an approach with the exchange of one or more Regge trajectories, corresponding to, in this reaction, K and K^* trajectories [1,2]. For a single trajectory, the cross section $d\sigma/dt$ can be parametrized as

$$d\sigma/dt = D(t)\left(\frac{s}{s_0}\right)^{2\alpha(t)-2}, \tag{1}$$

where s_0 is a scale factor taken to be 1 GeV and $D(t)$ is a function of t alone. $\alpha(t)$ is the Regge trajectory that describes how the angular momentum of the exchange varies with t. Note that in a reaction where $\alpha(t) \sim 0$, one would expect the cross section to "scale" with s^{-2}. That is, the s^2-scaled cross section would exhibit a uniform smooth dependence on $-t$ that depends neither on s nor separately on the production angle of the meson.

Exclusive scattering in the high-momentum and high-energy-transfer limit is thought to follow the constituent counting rules introduced in Refs. [3,4]. While the existence of these rules can be proved rigorously within perturbative QCD (pQCD) [3], they can also be derived based on more general grounds of the constituent nature of scattering without requiring the validity of pQCD [5]. In both interpretations, however, the onset of constituent counting manifests the transition from peripheral Regge-type scattering to short-range hard scattering involving a minimal number of partonic constituents, plus leptonic or photon fields, via which a given exclusive reaction can occur. The constituent counting rule predicts the analytical form for the differential cross section $d\sigma/dt$ to be

$$d\sigma/dt = f(t/s)s^{2-n} \tag{2}$$

in the limit that $s \gg M_i^2$ and t/s is fixed, where the M_i's are the masses of the particles involved in the reaction. The power factor n is the minimal number of pointlike constituents needed to accomplish the reaction. For photoproduction of pseudoscalar mesons, the relevant n is 9 if the photon is counted as a single elementary field, so the expectation is that the cross section should scale as s^{-7}. The requirement that t/s remain fixed at given high s amounts to the meson production angle, $\cos\theta_{\text{c.m.}}$, being held fixed. The form of the function f is not specified but can be in principle calculated either within pQCD or in nonperturbative models of constituent quark scattering. The major problem with pQCD, however, is in significant underestimation of the absolute magnitude of the function f (see, e.g., Ref. [6]). Note that in several instances the energy dependence of hard exclusive reactions can be reproduced within phenomenological models invoking only hadronic degrees of freedom (e.g., in Ref. [7]). In such models, however, the power law of the energy dependence is rather an accidental result. This situation cannot explain the "persistent" consistency of the constituent scaling law observed for many hard exclusive reactions including hadronic [8] and photoproduction [9] reactions, involving proton, deuteron, and even ^{3}He targets at $|t|, |u| > M_i^2$ kinematics (see, e.g., Refs. [10–12]). In the photoproduction case, s^{-7} scaling was found to be consistent with data for the final states π^+n, π^0p, $\pi^-\Delta^{++}$, ρ^0p, and (with poor statistics) for $K^+\Lambda$ and $K^+\Sigma^0$. The data in the present study are at W values covering the N^* resonance domain but with higher statistics than earlier work.

At kinematics similar to the reaction studied in the present paper, pion photoproduction at large angles exhibits s^{-7} scaling when the transverse momentum in the c.m. frame exceeds 1.2 GeV/c, as well as possible "oscillatory" features around the scaling prediction [13,14]. The former behavior has been interpreted as a clear signature for the onset of constituent scaling. The latter behavior has been discussed in terms of the breakdown of locality in quark-hadron duality that relates resonance excitations at low energies to parton phenomena at high energies [15]. The analogous KY behaviors have not previously been examined.

In the lower-energy domain of the nucleon resonances, that is, below $W = \sqrt{s} \sim 2.5$ GeV, several nonstrange

$I = 0$ baryon resonances contribute to the $\gamma + p \to K^+ + \Lambda$ reaction mechanism. So-called hadrodynamic models based on effective Lagrangians have, for many years, been employed with moderate success to describe a wide range of hadronic and electromagnetic reactions, including the particular reaction that is the focus of this paper [17–28]. Looking for such resonances in strangeness-containing final states has been a hunting ground for so-called "missing" resonances predicted in quark models [29] but not seen in pionic final-state experiments. Separating out the resonant contributions to the overall reaction mechanism has been pursued in various model approaches. In recent times, the most advanced methods include unitary coupled-channels methods that fit data sets from multiple channels simultaneously. For example, in the approach used by the Bonn-Gatchina group [20,21], the dominant partial waves in the present reaction of interest are consistent with $N(1720)P_{13}$, $N(1900)P_{13}$, $N(1840)P_{11}$, and an S_{11} wave. A problem with this and similar hadrodynamic approaches lies in the broad freedom in the overlap of several contributing N^* resonances and insufficient experimental constraints from spin observables to uniquely describe the reactions. As an alternative to the N^* resonance picture involving three-quark resonances, it has also been proposed [30,31] that the intermediate excitation in this reaction is a $K\overline{K}N$ structure that is dynamically generated in the rescattering of distinct mesons and baryons.

To address some of these issues, the CLAS Collaboration has published high-statistics cross-section data for the reaction $\gamma + p \to K^+ + \Lambda$ in recent years [32,33]. The earlier paper by Bradford *et al.* [32] showed that the cross section scales at low $-t$ with s^{-2}, consistent with the idea that $\alpha(t) \sim 0$ in this kinematic domain. Results in the more recent paper by McCracken *et al.* [33] are entirely consistent with the earlier paper but extend the range of W by about 300 MeV, to 2.8 GeV, and have improved statistical precision by a factor of about 4. This allows us to revisit the question of scaling and resonances outlined above.

This paper is organized first with more theoretical background about scaling in Sec. II, and then the experimental results demonstrating scaling behavior are shown in Sec. III. The apparent resonant aspects of the scaled data are presented in Sec. IV together with a model description. The results are discussed and summarized in Sec. V.

II. PARTONIC CONTENT OF THE REACTION

The onset of the energy scaling of the differential cross section of the $\gamma N \to MB$ photoproduction reaction in the form of s^{-N} at fixed $\cos\theta_{\rm c.m.}$ indicates in a certain degree the factorization of the hard subprocesses in the scattering amplitude, which can be expressed in the form (see, e.g., Refs. [3,34–36])

$$M^{\lambda}(s,t) = \int d^4[k_2]d[p_2]d^4[k_1]d[p_1]\psi^{\dagger}_M(k_2)\psi^{\dagger}_B(p_2) \times H^{\lambda}(p_2,k_2,p_1,k_1)\psi_{\gamma,\rm phys}(k_1)\psi_N(p_1), \quad (3)$$

where ψ_M, ψ_B, ψ_N, and $\psi_{\gamma,\rm phys}$ represent the soft partonic wave functions of the meson, produced baryon, initial nucleon, and physical photon, respectively. The kernel H represents the amplitude of the factorized hard-scattering subprocess which at asymptotic energies defines the *whole energy dependence* of the total scattering amplitude in the scaling form of $s^{-[(n-4)/2]}$, where $n = n_N + n_{\gamma,\rm phys} + n_M + n_B$ with n_N, $n_{\gamma,\rm phys}$, n_B, and n_M being the number of the partons (or elementary fields) entering in the wave function of the scattering particles. Note that at preasymptotic energies the above energy dependence is convoluted with the energy dependence following from the subleading as well as nonperturbative (resonating) processes. The latter can result in the additional oscillatory energy dependence of the s^N scaled differential cross sections (see, e.g., Refs. [37,38]).

While the number of the partonic constituents in the wave function of hadrons in Eq. (3) can be identified with that of the valence quarks, the interpretation of the physical photon at preasymptotic energies requires the consideration of both bare and hadronic components of its wave function. It is rather well established that the physical photon's wave function can be represented through the superposition of a bare photon and hadronic components (see, e.g., Ref. [39]):

$$\psi_{\gamma,\rm phys} = \psi_{\gamma} + \psi_{\rm hadron}, \quad (4)$$

where the hadronic part is dominated by intermediate vector meson states. Because of the large interaction cross section the hadronic part of the photon wave function dominates in many photoproduction processes, especially those involving the production of vector mesons.

In the high-energy and- momentum-transfer limit one expects that the bare photon component will gradually dominate in the photoproduction cross section since the hard kernel H involving the hadronic component of the photon is suppressed by an additional factor, $s^{-(1/2)}$, as compared to the amplitude involving the bare photon only. However, for the intermediate range of energies the hadronic component may still dominate in the hard processes at $|t|, |u| > M_N^2$ owing to the relatively large coupling constant of the physical photon to the vector mesons. In this case the hard rescattering (see, e.g., Ref. [40]) of intermediate vector mesons off the target nucleon defines the energy dependence of the photodisintegration cross section.

This situation can explain the observed s^{-8} scaling of hard real Compton scattering at large $\cos\theta_{\rm c.m.}$ [41,42] as well as exclusive photoproduction of $(\rho + \omega)$ mesons [9] which agrees reasonably well with the s^{-8} scaling of the differential cross section.

The situation, however, is simplified with consideration of the photoproduction of pseudoscalar mesons. In this case the contribution from $\psi_{\rm hadron}$ is suppressed since the dominating *vector meson* $+ N \to$ *pseudoscalar meson* $+ N'$ rescattering will proceed through the double helicity flip scattering, which one expects to be suppressed in the high-momentum-transfer limit. This expectation is confirmed in the exclusive photoproduction of π mesons in $\gamma N \to \pi N$ reactions, which clearly shows a s^{-7} scaling starting already at $s \approx 7$–8 GeV^2 [9,13,14].

Similar (early) scaling may be expected for kaon photoproduction in $\gamma + p \to K^+ + \Lambda$ or $\gamma + p \to K^+ + \Sigma^0$ reactions. The precision of the previous data [9] on exclusive kaon photoproduction was not sufficient (s^{-N}, $N = 7.3 \pm 0.4$)

to rule out unambiguously the contribution from the hadronic component of the photon wave function, which results in $N = 8$.

III. SCALING OF THE CROSS SECTION

Figure 1 shows the complete set of differential cross sections $d\sigma/dt$ from Ref. [33] versus $-t$. The published data were transformed from $d\sigma/d\cos\theta_{\rm c.m.}$ in the kaon production angle to $d\sigma/dt$ with the Jacobian $1/2kq$, where k is the initial-state c.m. momentum and q is the final-state c.m. momentum. The data are binned in bands of center-of-mass angle $\cos\theta_{\rm c.m.}$, each of width 0.1. Representative error bars are shown only for several angles important for this discussion; the close spacing of the data points makes it easy to trace the trends as a function of angle. The important observation here is that for forward angles (solid green points) the cross sections fall smoothly with increasing $-t$, and that there is some hint of "structure" for intermediate angles near $-t \sim 1.0$ GeV^2.

Figure 2 shows the same data with a scaling factor of s^2 applied. It is evident that the forward-angle data now fall on a fairly tight locus of points, while for $|-t| \geqslant 1.0$ GeV^2 this simple scaling fails. The scaling exponent of 2 is qualitatively optimal. The function $D(t) \sim e^{bt}$ in Eq. (1) has a slope estimated as $b = 3.0 \pm 0.7$ GeV^{-2}. Refining the effective Regge trajectory as per $\alpha(t) = \alpha_0 + \alpha' t$, and adjusting the value of $-t$ at which the trajectory "saturates," results in a somewhat tighter bunching of the loci of points, but for the present discussion we chose not to fine-tune this approach. This "Regge scaling" of the small $-t$ data simply confirms the observations made in Ref. [32].

The next question is to what degree the cross section satisfies the constituent counting rule expectation of s^{-7} scaling. The data for 90° are shown in Fig. 3 scaled by a floating power N as s^N. The choice of angle arises from where one expects scaling to be apparent at the lowest s while being farthest from small t and u. A fit was performed to optimize N, and the value of the scaled cross section is shown as the (red) horizontal bar. For $s > 5.0$ GeV^2 the CLAS data show a nearly flat behavior, while below this there are bumps due to resonance production (to be discussed in Sec. IV). The best-fit values to combined CLAS and SLAC data were found to be $N = 7.1 \pm 0.1$ and $s^N(d\sigma/dt) = 1.0 \pm 0.1$ nb GeV^{2N-2}, with $\chi^2/\nu = 92/60$. This is a fair-quality fit and strongly supports the validity of the s^{-7} hypothesis that hinges on counting the photon as a single bare elementary field. In the following discussion, we will take N to be exactly 7.0.

In the range of $5 < s < 8$ GeV^2 where the scaling is observed, the absolute cross section drops by a factor of 27, while the s^7-scaled cross section varies between 0.8 and 1.2. The onset of scaling at $s \approx 5.3$ GeV^2 corresponds to produced mass $W = 2.3$ GeV, and we note that almost all the data points in the present data set have transverse momentum in the center of mass, $p_\perp$, well below 1.0 GeV/c, averaging just 0.6 GeV/c.

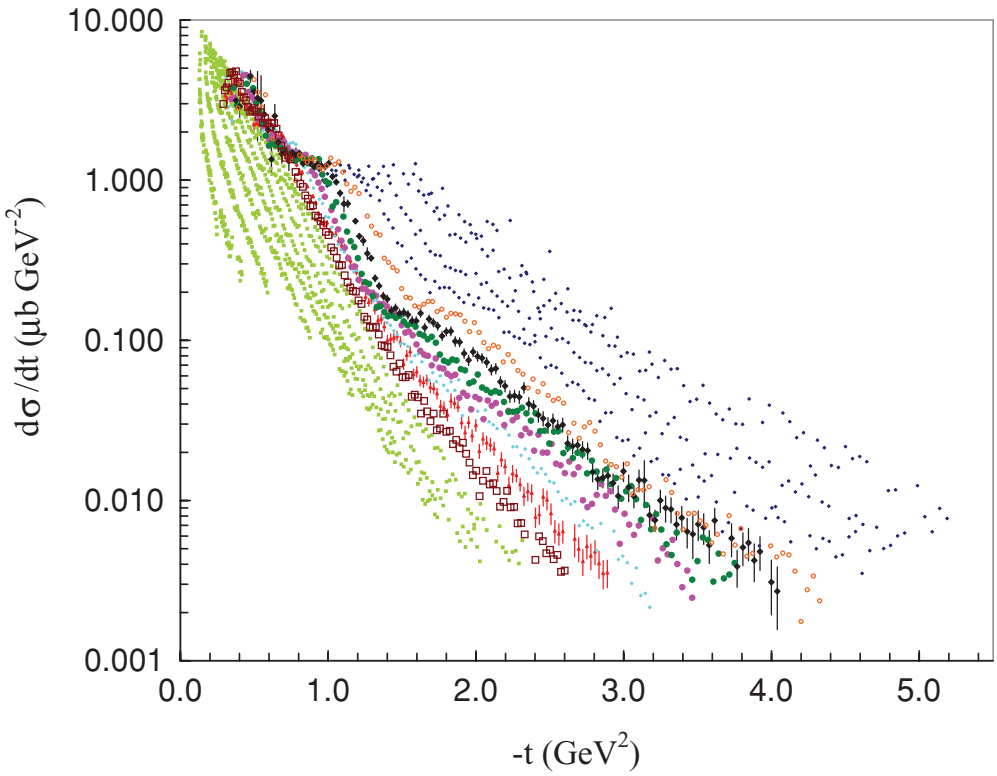

FIG. 1. (Color online) Cross section for the reaction $\gamma + p \to K^+ + \Lambda$ as a function of $-t$ with no scaling factors applied. Each band of points shows data for a bin in $\Delta\cos\theta_{\rm c.m.}$ of 0.1. Only a few specific bands have been highlighted with different colors. The color code is as follows: all forward-angle bands for $\cos\theta_K$ +0.9 to +0.2 (light green points), +0.1 (open brown squares), 0.0 (filled red triangles), −0.1 (filled cyan points), −0.2 (filled magenta circles), −0.3 (filled green squares), −0.4 (filled black diamonds), −0.5 (open orange circles), −0.6 to −0.9 (blue points). Representative statistical error bars are shown for only a few angle bands for clarity.

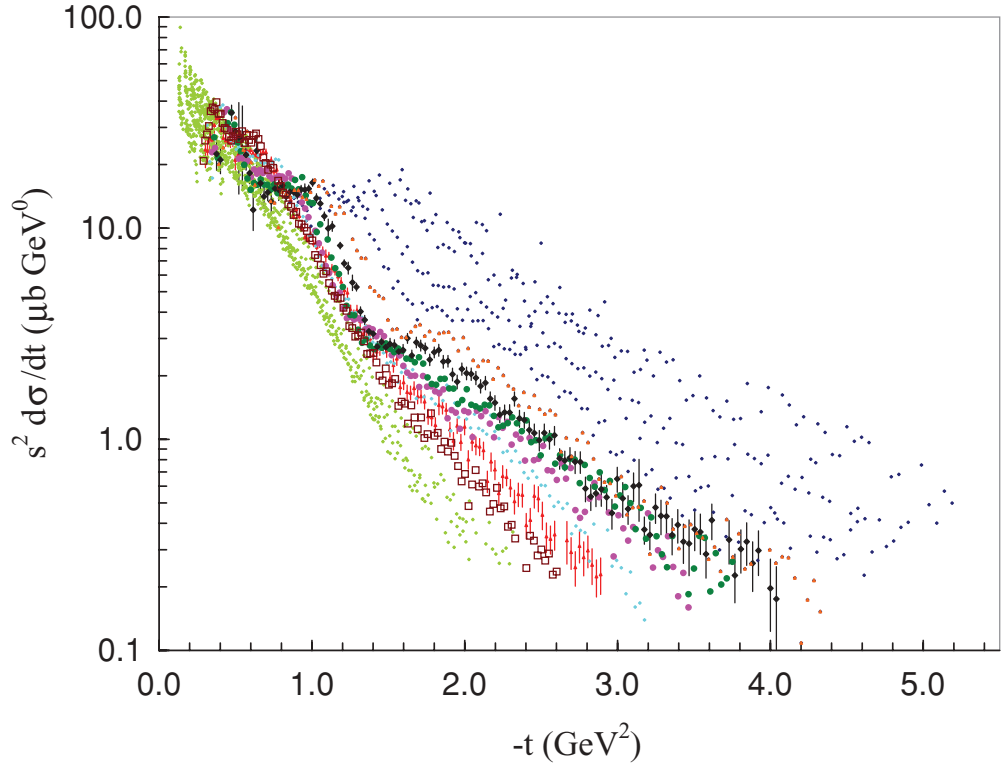

FIG. 2. (Color online) Cross section for the reaction $\gamma + p \to K^+ + \Lambda$ as a function of $-t$ with a scaling factor of s^2 applied. Note how the forward-angle points (light green) fall approximately on a single locus. The data and color coding are the same as for Fig. 1.

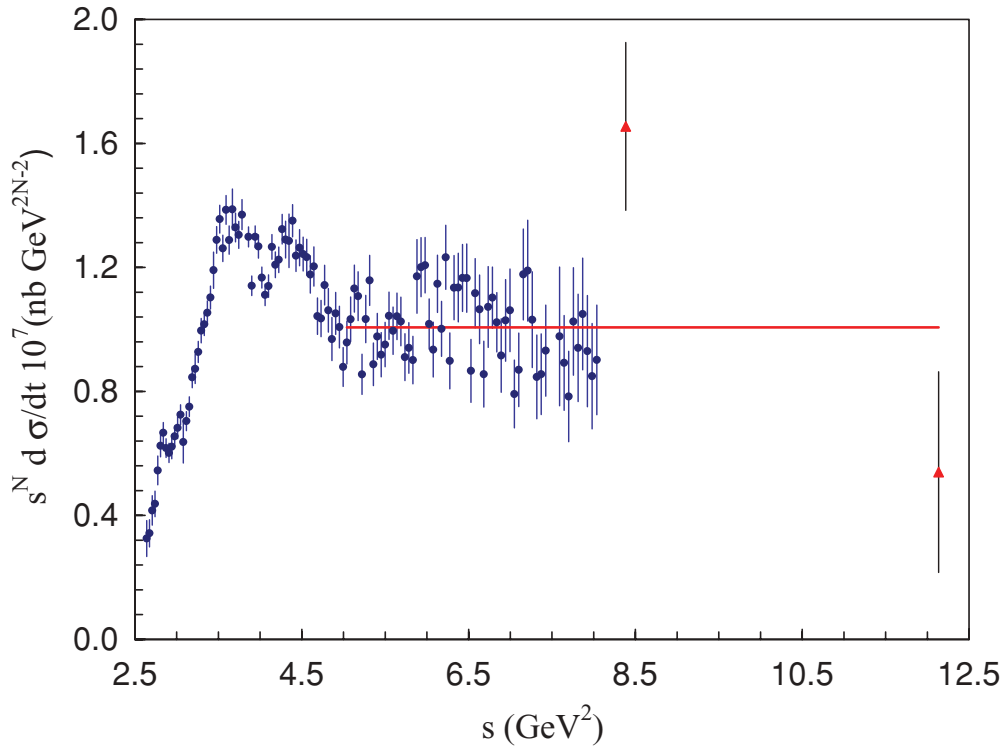

FIG. 3. (Color online) Cross section for the reaction $\gamma + p \to K^+ + \Lambda$ at 90° as a function of s with a scaling factor of s^N applied. CLAS data are solid (blue) circles [33], and SLAC data are (red) triangles [9]. The power-law fit [solid horizontal (red) line] is discussed in the text.

All these numbers indicate a much earlier onset of scaling as compared to the $\gamma N \to \pi N$ channels [13,14], for which the s^{-7} scaling sets in at $W \geqslant 2.7$ GeV and $p_\perp \geqslant 1.2$ GeV/c. This may indicate stronger convergence of the sum over produced strange hadron states leading to the earlier onset of the deep inelastic scattering regime relative to the case of nonstrange hadrons. Possible small variation around the scaled value in Fig. 3 suggests the validity of local duality [15,16]; however, the study of the latter is beyond the scope of this paper.

The evolution with energy of $f(t/s)$ in Eq. (2) is shown in Fig. 4. It presents the differential cross section scaled by s^7 as a function of $\cos\theta_{\rm c.m.}$. In the high-energy limit, wherein masses can be ignored, one has $-t/s = (1 - \cos\theta_{\rm c.m.})/2$. Under the present kinematics this not the case; for example, at 90° we have that $-t/s$ ranges from 0.12 to 0.36, not close to 0.5. Nevertheless, we use $\cos\theta_{\rm c.m.}$ as a proxy for $-t/s$ to test for scaling. Each connected band of points shows the weighted mean of the data in a range $\Delta W = 100$ MeV. The bands range from near threshold, centered at $W = 1.68$ GeV, to a maximum $W = 2.78$ GeV. It is evident that the forward-angle scaled cross section rises rapidly with energy but starts to plateau above about $W = 2.6$ GeV. For $\cos\theta_{\rm c.m.} < +0.5$, the bands converge when $W \geqslant 2.3$ GeV is reached. The intermediate range of angles, which we shall take to be from $+0.1$ in $\cos\theta_{\rm c.m.}$ to -0.5, shows a fairly tight band of scaled values at all W. The small error bars show that the spacing between the sets of points is very significant, and this energy dependence will be discussed in Sec. IV. The largest kaon production angles show a uniform rise in the scaled cross section, which we presume is evidence of u-channel contributions. The rise is less pronounced than what was observed in the πN channels but similar to that in the $\pi\Delta$ channels [9]. In comparison to previous data from SLAC [9] at $W = 2.9$ and 3.5 GeV, we see that the agreement is excellent; of course the recent CLAS data have greatly extended the precision and scope of angle and energy coverage.

The angular dependence is sensitive to the spin-isospin symmetry structure of the valence quark wave function of the hadrons entering in Eq. (3) (see, e.g., Refs. [35,36]). In the case of the photoproduction of pions, the amplitude probes the isospin-1/2 and -3/2 and helicity-1/2 combinations of the initial- and final-state partonic wave functions. The $\gamma p \to \pi^+ n$ scattering yields rather symmetric distribution around $\theta_{\rm c.m.} = 90°$, consistent with the *ad hoc* angular function [9]

$$f^{\gamma p \to \pi^+ n}(\cos\theta_{\rm c.m.}) = (1 - \cos\theta_{\rm c.m.})^{-5}(1 + \cos\theta_{\rm c.m.})^{-4}. \quad (5)$$

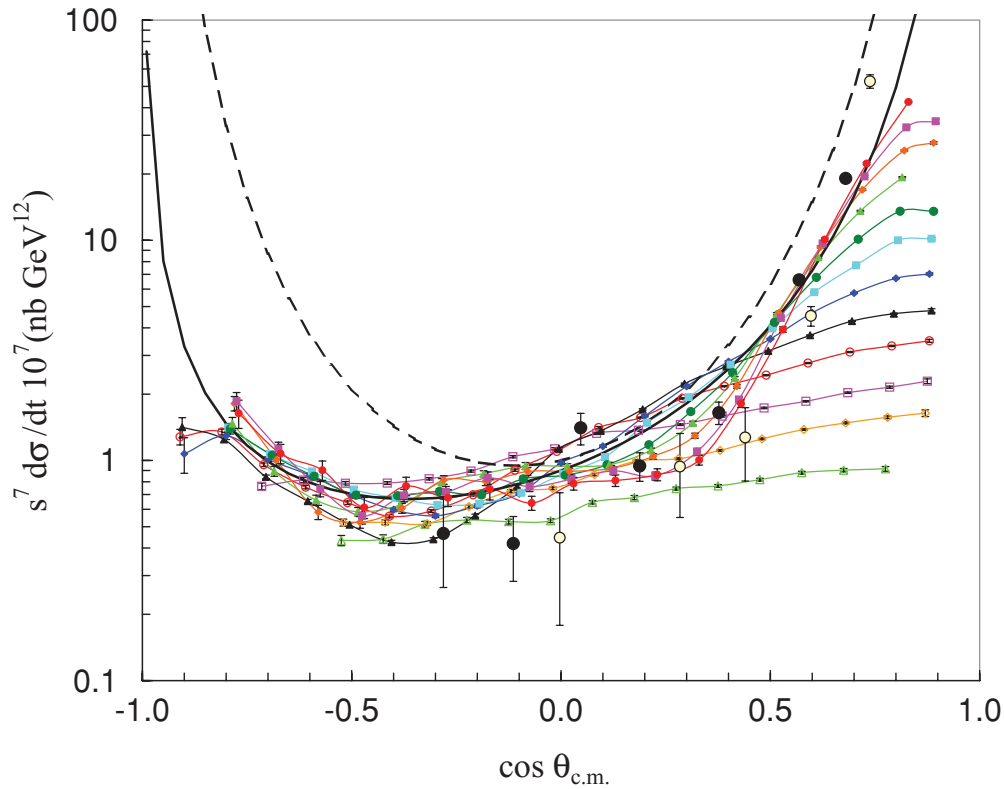

FIG. 4. (Color online) Scaled cross section versus center-of-mass meson production angle. Each connected string of data points represents a 100-MeV-wide band of W, where the color and symbol coding is easiest to see on the right-hand (forward-angle) side. From high to low: $W = 2.78$ GeV (solid red circles), 2.68 GeV (solid magenta squares), 2.58 GeV (solid orange diamonds), 2.48 GeV (solid light green triangles), 2.38 GeV (solid dark green circles), 2.28 GeV (solid cyan squares), 2.18 GeV (solid blue diamonds), 2.08 GeV (solid black triangles), 1.98 GeV (open red circles), 1.88 GeV (open magenta squares), 1.78 GeV (open orange diamonds), 1.68 GeV (open light green triangles). The CLAS data are the connected lines [33], with statistical errors that are usually smaller than the points. The SLAC data at $W = 2.9$ GeV are closed black circles, while 3.5-GeV data are open white circles [9]. The curves are explained in the text.

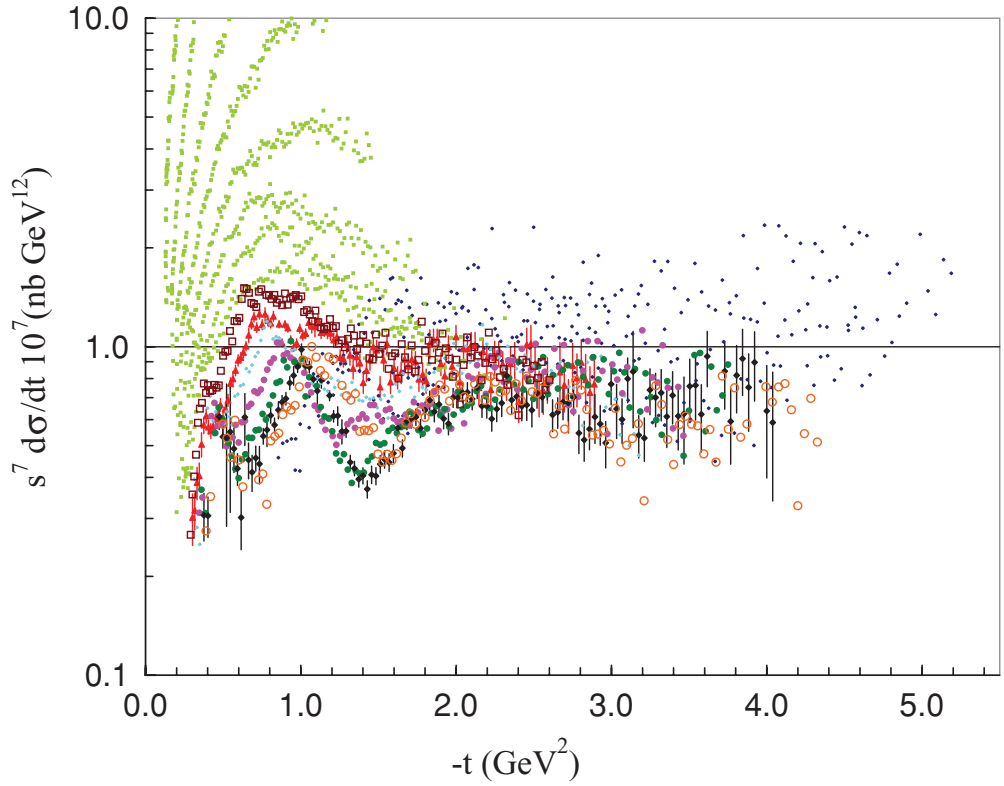

FIG. 5. (Color online) Cross section for the reaction $\gamma + p \to K^+ + \Lambda$ as a function of $-t$ with a scaling factor of s^7 applied. Note how the mid- and back-angle points (not light green) fall approximately on a single locus. The data and color coding are the same as for Fig. 1.

This is shown as the dashed line in Fig. 4. The present data on $\gamma p \to K^+\Lambda$ scattering, which exclude isospin-3/2 combinations, show a markedly different angular distribution consistent with

$$f^{\gamma p\to K^+\Lambda}(\cos\theta_{\rm c.m.}) = (0.9 \pm 0.1)(1 - \cos\theta_{\rm c.m.})^{-3.0\pm.2} \times (1 + \cos\theta_{\rm c.m.})^{-1.4\pm.1} \quad (6)$$

on a scale of 10^7 nb GeV^{12}. This is shown as the solid black line in Fig. 4. Evidently the t-channel (forward-angle) pieces of pion and kaon production are similar, while the u-channel (back-angle) portion of kaon production is weaker than for pion production. The s^7 scaling value of the cross section averaged across *all* intermediate angles is $(0.9 \pm 0.1) \times 10^7$ nb GeV^{12}. This numerical value is the same as the scaling value measured for $\gamma p \to \pi^+ n$ (see Refs. [9,13]). This similarity of the scaled cross-section values was first noted by Anderson *et al.* [9]. This can be understood within the framework of Eq. (3), according to which if $|t|, |u| \gg M_N^2, M_\Lambda^2$ such that all masses involved in the scattering can be neglected, the hard kernel should have similar structure for photoproduction of both pions and kaons. Combining these results with those for the $K^+\Sigma^0$ channel may allow us, for example, to constrain the relative weight of the vector and scalar diquarks in the nucleon wave function (see, e.g., Refs. [35,36]). In summary, one may say that the scaling function $f(t/s \to \simeq \cos\theta_{\rm c.m.})$ is approaching an energy-independent shape for W greater than $\approx$2.6 GeV, but there remain significant $\sim\pm$30% variations with energy at all angles.

Figure 5 again shows the whole data set scaled by s^7 but versus $-t$. The light green forward-angle data above about 1.6 on the vertical axis are now "overscaled," with clear positive-sloped bands corresponding in order from high to low values of $\cos\theta_{\rm c.m.}$ of $\{0.9, 0.8, \ldots, 0.2\}$. These forward-angle bands were the ones that showed the $N = 2$ Regge scaling discussed above, so they clearly cannot also exhibit $N = 7$ scaling. The intermediate-angle data, however, do fall on a roughly constant locus of points. These intermediate angles are color coded for each angle bin as in Figs. 1 and 2, spanning the range $\cos\theta_{\rm c.m.} = \{+0.1, 0.0, -0.1, \ldots, -0.5\}$ for all W. Beside the overall s^{-7} scaling of the intermediate-angle cross sections, the other striking feature of the scaled data in Fig. 5 is their oscillatory angle-dependent aspect between $\cos\theta_{\rm c.m.}$ of $+0.1$ and -0.5 for values of $-t$ from essentially zero to -2.0 GeV^2. This behavior with angle seems to strongly suggest the interference of resonant amplitudes. Since the bump structure does not occur at fixed $-t$, in Sec. IV we look instead at the structure as a function of the invariant center-of-mass energy W.

IV. RESONANCE CONTENT OF THE REACTION

Figure 6 shows the scaled cross section again but plotted versus W and on a linear scale. The high-statistics forward-angle points for $\cos\theta_{\rm c.m.} \geqslant +0.2$ (solid light green, mostly above 1.6 on the vertical scale) are now mapped across all W and will henceforth be ignored, since they clearly do not follow the s^{-7} scaling trend. Also, we similarly will ignore the

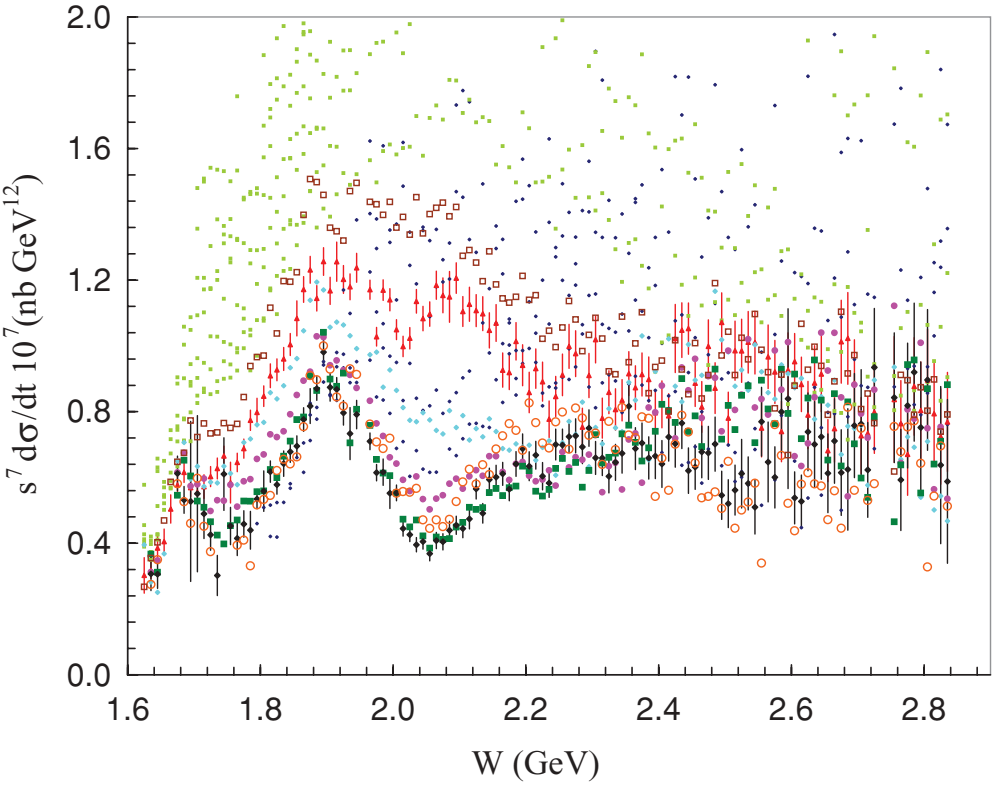

FIG. 6. (Color online) Cross section for the reaction $\gamma + p \to K^+ + \Lambda$ as a function of W with a scaling factor of s^7 applied. Note how the mid- and back-angle bands of points (all but light green) form distinctive features. The vertical scale is now linear rather than logarithmic. The data and color coding are the same as for Fig. 1. Representative statistical error bars are shown for several angle bands only.

low-statistics data at the largest production angles (blue points) because of their low precision. The main observation here is that the oscillatory and interferencelike structures are now well aligned near $W = 1.7$, 1.9, and 2.1 GeV. This suggests that these structures are caused by s-channel resonance production and interference. The s^7 scaling has brought these structures into sharp relief, even though they are clearly present also in the unscaled data if one looks carefully [33]. The origin of the major peak at $W = 1.9$ GeV has been a source of debate for years, while the structure near 2.1 GeV has gone unnoticed. Resonance peaks at low W were observed previously in s^7-scaled pion photoproduction [13,14], including an unexplained broad enhancement near 2.1 GeV (see Ref. [13] and Fig. 3). But the present study is the first to discuss an angle-dependent interference structure superimposed on the flat scaling plateau in hyperon production.

To investigate the nature of the resonance content seen in this reaction, the following model of interfering resonance states was developed to compare to the data. Each N^* resonance was modeled with a relativistic Breit-Wigner amplitude written as

$$\mathrm{BW}_{J_z}(m) = \frac{\sqrt{m m_0 \Gamma_{J_z,\gamma p\to N^*}\Gamma_{N^*\to K\Lambda}(q)}}{m^2 - m_0^2 - i m_0 \Gamma_{\mathrm{tot}}(q)}, \tag{7}$$

where $m = \sqrt{s}$ is the running mass value, m_0 is the centroid mass of the resonance, and $q = q(m)$ is the c.m. frame momentum of the $K^+\Lambda$ final state. The decay width to the final state was written

$$\Gamma_{N^*\to K\Lambda} = \Gamma_0 \left(\frac{q}{q_0}\right)^{2L+1}, \tag{8}$$

where L is the orbital angular momentum of the decay and q_0 is the c.m. momentum at the resonance centroid energy. The nominal decay width Γ_0 was taken as an adjustable parameter. The photo coupling to the N^* state in spin projection J_z, $\sqrt{\Gamma_{J_z,\gamma p\to N^*}}$, was taken as a complex parameter. The total width appearing in Eq. (7) was

$$\Gamma_{\mathrm{tot}}(q) = \Gamma_{N^*\to K\Lambda}(q) + \Gamma_S(q), \tag{9}$$

where $\Gamma_S(q)$ was designed to enforce the s^{-7} scaling seen in the data. Without extra damping of the high-mass tails of the Breit-Wigner line shapes, the computed cross-section fits failed utterly to reproduce the scaling. Physically this may correspond to the channel coupling and unitarity bounds that are ignored in this model. Therefore, an extra width, $\Gamma_S(q)$, was introduced in the form

$$\Gamma_S = \Gamma_{S_0}\left(\frac{q}{q_S}\right)^7. \tag{10}$$

The reason for the power 7 in this expression is that at high energy $q \to (1/2)\sqrt{s}$. In the square of the matrix element, therefore, the line shape scales asymptotically as s^{-7}. The parameter Γ_{S_0} was fitted to be 0.50 GeV, which is the same as the widths of the four-star resonances in the 2- to 2.5-GeV mass region. The scale q_S was a free parameter, chosen to make the

highest-W portion of the curves have the correct behavior. The value turned out to be 0.77 GeV, which is larger than the values of q_0 for any of the resonances included in the model. Thus, this phenomenological damping of the Breit-Wigner mass tails has an effect at the high end of the mass distribution and has little effect in the region where the angle-dependent scaled cross section is prominent.

Using the beam axis as the quantization axis, each resonance was allowed to couple to the unpolarized initial photon and proton states via total spin projection $J_z = 1/2$ and $3/2$. The final orbital states that were allowed were $L = 0,\ 1$, and 2. For example, the final state amplitude $\psi_L(J, J_z)$ of a $J = 3/2$ resonance formed through the $J_z = 1/2$ initial spin projection and that decayed to a P-wave final state was written as

$$\psi_P\left(\tfrac{3}{2}, +\tfrac{1}{2}\right) = \left\{\tfrac{1}{\sqrt{3}} Y_{1,1}\alpha_{\frac{1}{2},-\frac{1}{2}} + \sqrt{\tfrac{2}{3}} Y_{1,0}\alpha_{\frac{1}{2},+\frac{1}{2}}\right\} \mathrm{BW}_{1/2}(m), \tag{11}$$

where the $Y_{L,M}$'s are the spherical harmonics, and the α_{J,J_z}'s are the nucleon spinors. Analogous expressions define the other final-state amplitudes used: $\psi_P(3/2, +3/2)$, $\psi_D(3/2, +1/2)$, $\psi_D(3/2, +3/2)$, and $\psi_S(1/2, +1/2)$. The total angular intensity distribution as a function of $W(= \sqrt{s} = m)$ and production angle was then computed according to

$$|A(m, \cos\theta_{c.m.})|^2 = \left|\psi_S\left(\tfrac{1}{2}, +\tfrac{1}{2}\right) + \psi_P\left(\tfrac{3}{2}, +\tfrac{1}{2}\right) + \psi_P\left(\tfrac{3}{2}, +\tfrac{3}{2}\right) + \psi_D\left(\tfrac{3}{2}, +\tfrac{1}{2}\right) + \psi_D\left(\tfrac{3}{2}, +\tfrac{3}{2}\right)\right|^2, \tag{12}$$

where we allow for a single S-wave, P-wave, and D-wave resonance only.

The unscaled cross section was computed using

$$\frac{d\sigma}{d\cos\theta_{\mathrm{c.m.}}}(W, \cos\theta_{\mathrm{c.m.}}) = \frac{(\hbar c)^2}{32\pi}\frac{1}{s}\frac{q}{k}|A|^2, \tag{13}$$

where the only additional factor is k, the initial-state center-of-mass momentum. This cross section was then converted to $d\sigma/dt$ and scaled by s^7, as before.

Various combinations of total J and decay waves were tested to find a reasonable representation of the data. The most successful combination is shown in Fig. 7. The large- and small-angle data points have now been suppressed, as justified above, and the intermediate-angle data are shown together with the corresponding line shapes from the parametrization given above. The best combination of waves found was an S_{11} resonance near threshold, a P_{13} resonance centered at 1.92 GeV, and a D_{13} resonance centered at 2.10 GeV. Other combinations of waves with various values of L and J were tested, but each of those resulted in unacceptable angular distributions. For the high-mass D_{13} state at 2.10 GeV, alternatives tested were P_{13}, P_{11}, S_{11}, and D_{15}. The final tabulated values for the centroids, widths, and couplings are given in Table I, together with an estimate of the uncertainties. The photo couplings are given as the magnitude in $(\mathrm{GeV})^{1/2}$ and phase in degrees, as specified in Eq. (7). These values are the result of exploratory fits for a single reaction channel, with

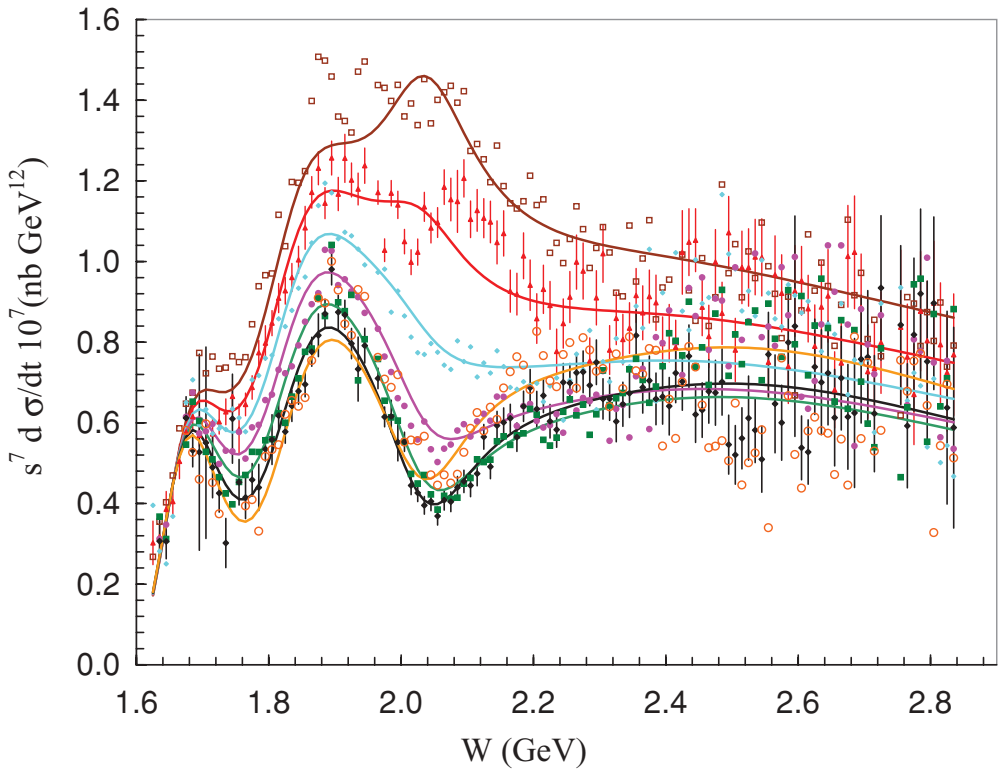

FIG. 7. (Color online) Cross section for the reaction $\gamma + p \to K^+ + \Lambda$ as a function of W with a scaling factor of s^7 applied, with model curves discussed in the text. The color code is as follows: $\cos\theta_{\mathrm{c.m.}} = +0.1$ (open brown squares), 0.0 (filled red triangles), -0.1 (filled cyan points), -0.2 (filled magenta circles), -0.3 (filled green squares), -0.4 (filled black diamonds), and -0.5 (open orange circles). Representative statistical error bars are shown for several angle bands only.

TABLE I. Results for the resonant content fitted to the scaled cross section. The masses and widths are for the fitted relativistic Breit-Wigner functions. The overall phases are specified relative to the P_{13} state.

Resonance and decay	m_0 (GeV)	Γ_0 (MeV)	$\sqrt{\Gamma_{1/2,\gamma p\to N^*}}$ $(\mathrm{GeV})^{1/2}$ phase	$\sqrt{\Gamma_{3/2,\gamma p\to N^*}}$ $(\mathrm{GeV})^{1/2}$ phase
S_{11}	1690 ± 10	80 ± 20	1.83 ± 0.10 $(-142 \pm 5)^\circ$	
P_{13}	1920 ± 10	440 ± 100	1.93 ± 0.10 –	$1.67 \pm .07$ –
D_{13}	2100 ± 20	200 ± 50	0.61 ± 0.10 $(45 \pm 5)^\circ$	$1.19 \pm .10$ $(45 \pm 5)^\circ$

possible finer details in the data not reproduced. For instance, we did not include the $N(1720)P_{13}$ that is established [21] in multichannel fits but is not dominant near threshold. The identification of the principal resonant components in the fits seems secure, however. In particular, taking the state at 1.9 GeV to be P_{13} leads to the state at 2.1 GeV being strongly favored as D_{13}.

Figure 8 shows the final line shapes again but with the underlying resonance shapes included. Note the long tails on each modified Breit-Wigner curve that arise from the interplay of the scaling by s^7 and the damping width specified in Eq. (10).

V. DISCUSSION AND CONCLUSIONS

We have discussed three features of the $\gamma + p \to K^+ + \Lambda$ reaction. First, we have confirmed [32], with higher statistics [33], the Regge-domain scaling with the power s^{-2} for the low-t data. Second, we have shown that the constituent counting rule prediction of s^{-7} scaling is quite well satisfied for this reaction for $|-t| \geqslant 2\ \mathrm{GeV}^2$, $W \geqslant 2.3$ GeV, and $p_\perp \geqslant 0.8\ \mathrm{GeV}/c$. These values are much lower than those observed for πN photoproduction. The scaled cross sections for $\pi^+ n$ and $K^+\Lambda$ are equal at 90°, but the angular dependencies away from 90° differ (Fig. 4). Quantitative analysis of this scaling based on QCD models or an alternative description based on unitary channel coupling remains to be investigated.

Third, we have shown that the scaled cross section at low to moderate $-t$ and $W < 2.3$ GeV shows structure consistent with the interference of a set of s-channel resonances. We make the ansatz that the scaled cross section can be analyzed with interfering Breit-Wigner resonance line shapes with the introduction of an empirical damping factor to achieve the s^{-7} scaling limit; the qualitative appearance of the data suggests this is reasonable. With this assumption, the best match to the data was found to include an $N(1690)S_{11}$, an $N(1920)P_{13}$, and an $N(2100)D_{13}$ suite of resonances. We remark that recent work by several groups using various effective Lagrangian formulations has consistently required an S wave near threshold and either a P or D wave near 1.9 GeV. The present work shows that the structure at 1.9 GeV is consistent with a P_{13} state. No previous work has made a

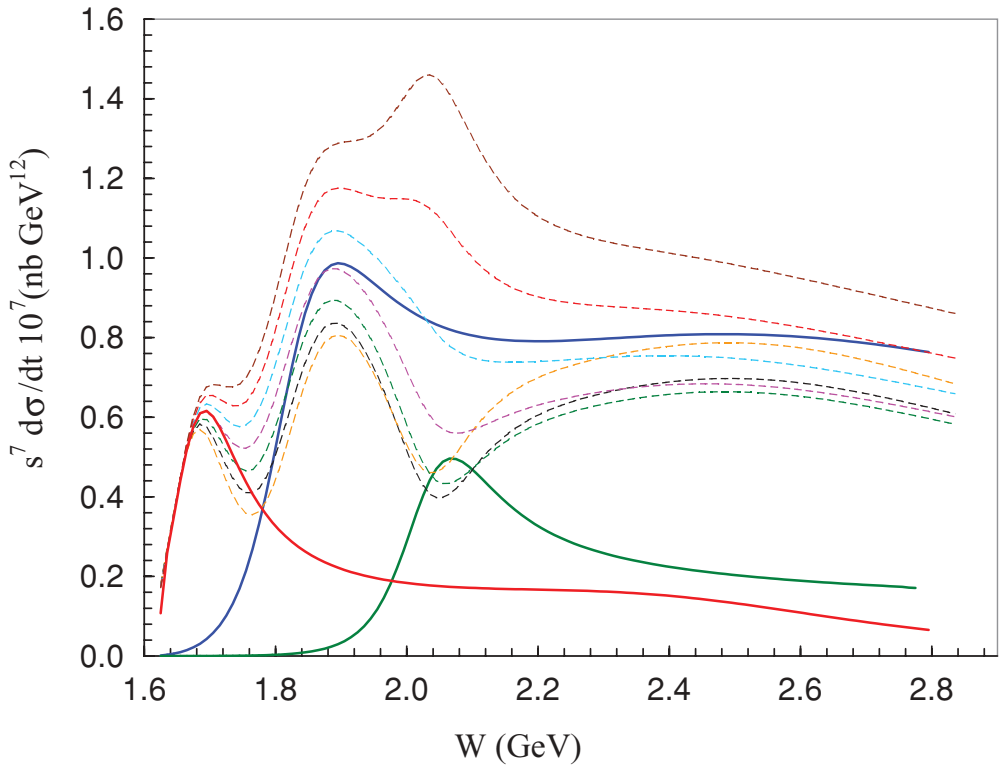

FIG. 8. (Color online) Phenomenological model for the reaction $\gamma + p \to K^+ + \Lambda$ as a function of W with a scaling factor of s^7 applied. The upper dashed curves are for individual angles as in Fig. 7, while the lower curves show the components: S wave (solid red), P wave (solid blue), and D wave (solid green).

claim for a D-wave structure near 2.1 GeV in this reaction channel; previously, data were too sparse to clearly examine the angular dependence in this mass range. From Fig. 8 one sees that this state influences the reaction also below 2 GeV. Hence, earlier work that concentrated on W below 2 GeV may need revision. We also note that the "two-star" [43] resonance $N(2080)D_{13}$ was identified by Capstick and Roberts [29] in their relativized quark model as having large combined strength in both photo coupling and decay to $K\Lambda$. This led Mart and Bennhold [27] to tentatively identify this state with the large structure at 1.9 GeV. Our study supports the existence of a D_{13} state coupling to $K^+\Lambda$, not at 1.9 GeV but rather at 2.1 GeV.

In this paper we have ignored the available spin observables for this reaction, including the recoil polarization of the Λ hyperon, P_Λ [33,44], the beam asymmetry Σ [47], the beam-recoil double polarizations C_x and C_z [45,46], and the beam-recoil linear double polarizations O_x and O_z [48]. Including these in amplitude-level fits results in much more sensitivity to smaller contributions to the reaction mechanism. Further, we have ignored the effects of unitarity bounds and channel coupling. Thus, the main result of this work has been to demonstrate how two different types of scaling apply to this reaction and to demonstrate how the s^7-scaled cross section highlights some of the important resonance contributions to the reaction mechanism.

This phenomenological analysis of the $\gamma + p \to K^+ + \Lambda$ reaction has thus yielded some insights into this reaction. However, a theoretical foundation for using the notions of s^{-7} scaling and baryon resonance analysis in the same framework is lacking. With the observations made here, we hope to stimulate further efforts to understand whether this approach can be put on a more rigorous footing. We expect to study other meson photoproduction reactions to test the consistency of this approach.

ACKNOWLEDGMENTS

This work was supported by US Department of Energy Grants No. DE-FG02-87ER40315 and No. DE-FG02-01ER41172.

[1] M. Guidal, J.-M. Laget, and M. Vanderhaeghen, Nucl. Phys. A **627**, 645 (1997).
[2] M. Guidal, J.-M. Laget, and M. Vanderhaeghen, Phys. Rev. C **61**, 025204 (2000).
[3] S. J. Brodsky and G. R. Farrar, Phys. Rev. Lett. **31**, 1153 (1973); Phys. Rev. D **11**, 1309 (1975); G. P. Lepage and S. J. Brodsky, *ibid.* **22**, 2157 (1980).
[4] V. A. Matveev, R. M. Muradian, and A. N. Tavkhelidze, Lett. Nuovo Cimento **7**, 719 (1973).
[5] N. Isgur and C. H. Llewellyn Smith, Nucl. Phys. B **317**, 526 (1989).
[6] G. R. Farrar, K. Huleihel, and H. Y. Zhang, Nucl. Phys. B **349**, 655 (1991).
[7] J. M. Laget, Phys. Lett. B **685**, 146 (2010).
[8] C. G. White *et al.*, Phys. Rev. D **49**, 58 (1994).
[9] R. L. Anderson *et al.*, Phys. Rev. D **14**, 679 (1976).
[10] C. Bochna *et al.* (E89-012 Collaboration), Phys. Rev. Lett. **81**, 4576 (1998).
[11] M. Mirazita *et al.* (CLAS Collaboration), Phys. Rev. C **70**, 014005 (2004).
[12] I. Pomerantz *et al.* (JLab Hall A Collaboration), Phys. Lett. B **684**, 106 (2010).
[13] W. Chen *et al.* (Jefferson Lab CLAS Collaboration), Phys. Rev. Lett. **103**, 012301 (2009).
[14] L. Y. Zhu *et al.* (Jefferson Lab Hall A Collaboration), Phys. Rev. Lett. **91**, 022003 (2003).
[15] Q. Zhao and F. E. Close, Phys. Rev. Lett. **91**, 022004 (2003).
[16] W. Melnitchouk, R. Ent, and C. Keppel, Phys. Rep. **406**, 127 (2005).
[17] A. V. Sarantsev, V. A. Nikonov, A. V. Anisovich, E. Klempt, and U. Thoma, Eur. Phys. J. A **25**, 441 (2005).
[18] A. Anisovich, E. Klempt, A. Sarantsev, and U. Thoma, Eur. Phys. J. A **24**, 111 (2005).
[19] A. V. Anisovich, A. V. Sarantsev, O. Bartholomy, E. Klempt, V. A. Nikonov, and U. Thoma, Eur. Phys. J. A **25**, 427 (2005).
[20] V. A. Nikonov, A. V. Anisovich, E. Klempt, A. V. Sarantsev, and U. Thoma, Phys. Lett. B **662**, 245 (2008).
[21] A. V. Anisovich, E. Klempt, V. A. Nikonov, A. V. Sarantsev, and U. Thoma, arXiv:1009.4803 [hep-ph].
[22] S. Janssen, J. Ryckebusch, D. Debruyne, and T. Van Cauteren, Phys. Rev. C **65**, 015201 (2001); S. Janssen *et al.*, Eur. Phys. J. A **11**, 105 (2001).
[23] S. Janssen, D. G. Ireland, and J. Ryckebusch, Phys. Lett. B **562**, 51 (2003).
[24] D. G. Ireland, S. Janssen, and J. Ryckebusch, Nucl. Phys. A **740**, 147 (2004).
[25] T. Corthals, J. Ryckebusch, and T. Van Cauteren, Phys. Rev. C **73**, 045207 (2006).
[26] B. Saghai, AIP Conf. Proc. **59**, 57 (2001); J. C. David, C. Fayard, G. H. Lamot, and B. Saghai, Phys. Rev. C **53**, 2613 (1996).
[27] T. Mart and C. Bennhold, Phys. Rev. C **61**, 012201(R) (1999).
[28] T. Mart, C. Bennhold, H. Haberzettl, and L. Tiator, KAONMAID 2000 [wwwkph.kph.uni-mainz.de/MAID/kaon].
[29] S. Capstick and W. Roberts, Phys. Rev. D **58**, 074011 (1998), and references therein.
[30] A. Martinez Torres, K. P. Khemchandani, U. G. Meissner, and E. Oset, Eur. Phys. J. A **41**, 361 (2009).
[31] D. Jido and Y. Kanada En'yo, Chin. Phys. C **33**, 1312 (2009).
[32] R. Bradford *et al.* (CLAS Collaboration), Phys. Rev. C **73**, 035202 (2006).
[33] M. E. McCracken *et al.* (CLAS Collaboration), Phys. Rev. C **81**, 025201 (2010).
[34] D. W. Sivers, S. J. Brodsky, and R. Blankenbecler, Phys. Rep. **23**, 1 (1976).
[35] P. Kroll, M. Schurmann, K. Passek, and W. Schweiger, Phys. Rev. D **55**, 4315 (1997).
[36] C. G. Granados and M. M. Sargsian, Phys. Rev. Lett. **103**, 212001 (2009).
[37] S. J. Brodsky and G. F. de Teramond, Phys. Rev. Lett. **60**, 1924 (1988).

[38] B. Pire and J. P. Ralston, Phys. Lett. B **117**, 233 (1982).
[39] T. H. Bauer, R. D. Spital, D. R. Yennie, and F. M. Pipkin, Rev. Mod. Phys. **50**, 261 (1978); **51**, 407(E) (1979).
[40] L. L. Frankfurt, G. A. Miller, M. M. Sargsian, and M. I. Strikman, Phys. Rev. Lett. **84**, 3045 (2000).
[41] A. Danagoulian *et al.* (Hall A Collaboration), Phys. Rev. Lett. **98**, 152001 (2007).
[42] L. Y. Zhu *et al.* (Jefferson Lab Hall A Collaboration), Phys. Rev. Lett. **91**, 022003 (2003).
[43] K. Nakamura *et al.* (Particle Data Group), J. Phys. G **37**, 075021 (2010).
[44] J. W. C. McNabb *et al.* (CLAS Collaboration), Phys. Rev. C **69**, 042201 (2004).
[45] R. Schumacher, Eur. Phys. J. A **35**, 299 (2008).
[46] R. Bradford *et al.* (CLAS Collaboration), Phys. Rev. C **75**, 035205 (2007).
[47] R. G. T. Zegers *et al.* (LEPS Collaboration), Phys. Rev. Lett. **91**, 092001 (2003).
[48] A. Lleres *et al.*, Eur. Phys. J. A **31**, 79 (2007).